Mesoscopic Rydberg ensembles: Beyond the pairwise-interaction approximation

K. C. Younge,[1,*] A. Reinhard,[1,†] T. Pohl,[2,3] P. R. Berman,[1] and G. Raithel[1]
[1]*Department of Physics, FOCUS Center and Michigan Center for Theoretical Physics, University of Michigan, Ann Arbor, Michigan 48109, USA*
[2]*ITAMP, Harvard-Smithsonian Center for Astrophysics, 60 Garden Street, Cambridge, Massachusetts 02138, USA*
[3]*Max Planck Institute for the Physics of Complex Systems, Nöthnitzer Straße 38, 01187 Dresden, Germany*
(Received 28 August 2008; published 27 April 2009)

We examine state mixing in a dense, cold Rydberg gas. Cold Rb atom clouds in an optical dipole trap are excited into $nD_{5/2}$ Rydberg levels using narrow-bandwidth laser pulses. For $n=43$, two atoms excited to $43D_{5/2}$ states can be converted to $41F_{7/2}$ and $45P_{3/2}$ product states via a Förster resonance. We find, unexpectedly, that up to 50% of the Rydberg atoms are detected in such product states after only 100 ns of interaction time. The experiment is modeled using many-body quantum simulations. To reproduce the mixing fractions measured near Förster resonances, we use an exact, nonperturbative many-atom Hamiltonian in which product states are treated on an equal basis with the laser-excited $nD_{5/2}$ Rydberg level. Simplified many-body interaction models based on sums over pairwise atomic potentials cannot reproduce the measured mixing fractions.

DOI: 10.1103/PhysRevA.79.043420 PACS number(s): 32.80.Rm, 03.67.−a, 34.20.Cf

I. INTRODUCTION

Systems of cold interacting Rydberg atoms have generated considerable interest over the past decade because of their strong interactions and collective, many-body properties. More recently, both experimental [1–5] and theoretical [6–8] studies have been carried out to probe the unique properties of Rydberg gases obtained by photoexcitation of laser-cooled cold atom clouds. Rydberg atoms can experience strong, near-resonant energy-exchange interactions, leading to population of states dipole coupled to the initially excited Rydberg level. Such energy-exchange resonances, often termed Förster resonances [9], are relevant in a number of important contexts including biological systems [10], nanophotonics [11], and quantum information processing applications [12]. In addition, interesting dynamics can occur in Rydberg systems in which there is an interaction-induced blockade of Rydberg excitation. Excitation suppression observed in dense Rydberg gases [3,13] has been modeled in terms of pairwise, additive Rydberg-Rydberg atom interactions [2,3,14,15].

In this paper we show that many-body nonadditive interactions can profoundly affect the dynamics of dense Rydberg gases. We study internal-state dynamics by monitoring the amount of state mixing near Förster resonances. Such resonances have been experimentally investigated for several Rydberg states using atoms stored in magneto-optical traps (MOTs) [13,16–20]. Here we implement a broadband optical dipole trap [see Fig. 1(a)] to achieve considerably higher densities that afford stronger interatomic interactions. In the vicinity of Förster resonances we observe strong state mixing. The mixing cannot be explained with commonly used models, in which the Rydberg-Rydberg interactions are described by a sum of pairwise level shifts. Instead, a treatment based on a nonperturbative, complete many-body Hamiltonian is required.

The many-body dynamics of rubidium atom clouds studied in this experiment originates in the interaction channel

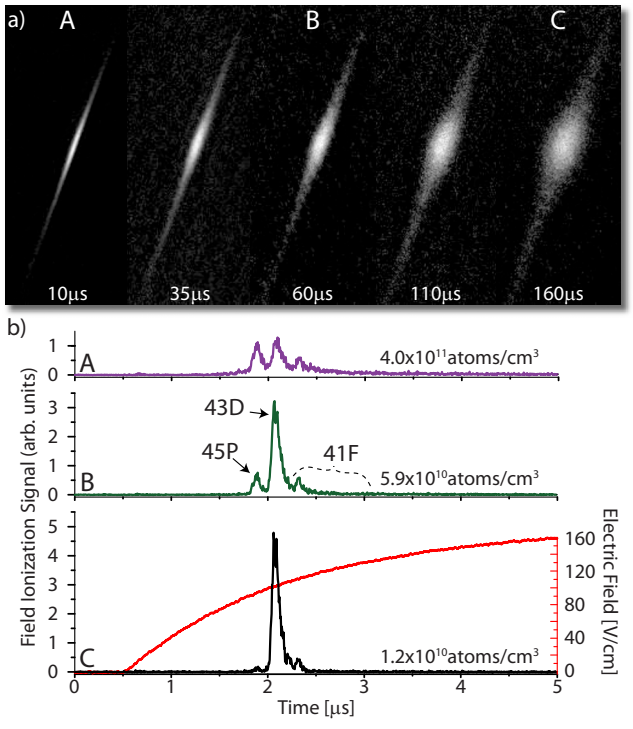

FIG. 1. (Color online) Trap images and corresponding field ionization signals for varying trap densities. (a) Shadow images of the dipole trap for expansion times ranging from 10 μs to 160 μs. Extending the expansion time allows the trap density to be continuously varied. Densities shown range from approximately 1×10^{10} cm^{-3} to 4×10^{11} cm^{-3}. (b) State-selective field ionization (SSFI) signals for (a) high, (b) intermediate, and (c) low density. The SSFI electric field ramp is shown on the right axis. The signals are normalized to equalize the area under each curve.

*kyounge@umich.edu
†Present address: The Pennsylvania State University, Department of Physics, 104 Davey Lab, University Park, PA 16802, USA.

$$nD_{5/2} + nD_{5/2} \leftrightarrow (n-2)F_{7/2} + (n+2)P_{3/2}, \quad (1)$$

where n is the principal quantum number. The reaction has an energy defect $\hbar\Delta$, defined as the energy of the two product (P and F) states minus the energy of the initial (D) states. The strength $V_{ij} = \mu_{dp}\mu_{df}/4\pi\varepsilon_0\hbar r_{ij}^3$ of the excitation exchange reaction is determined by the respective dipole transition elements μ_{dp} and μ_{df} and the distance r_{ij} between the atoms. The case of resonant coupling occurs at $n=43$, where the energy defect is only $-h\times 8$ MHz, and hence considerably smaller than the dipole coupling at typical interatomic distances. The dipole-dipole coupling can result in large energy level shifts

$$U_{ij} = \frac{1}{2}[|\Delta| - \sqrt{\Delta^2 + 8V_{ij}^2}] \quad (2)$$

of two interacting Rydberg atoms. Such level shifts inhibit simultaneous excitation of close atom pairs [12], and thus cause suppression of Rydberg excitation in cold gases, as observed for off-resonant van der Waals interactions [3] as well as Förster resonant interactions [13]. These observations are commonly explained by generalizing the above two-atom consideration to a gas of many atoms, whose second excited state is shifted by an amount given by a sum of binary, or pairwise, interaction potentials [Eq. (2)] [2,3,14,15]. Here we provide experimental and theoretical evidence that such approaches are insufficient in the vicinity of Förster resonances. Both resonant dipole-dipole ($\Delta \ll V_{ij}$) and nonresonant van der Waals ($\Delta \gg V_{ij}$) interactions are investigated by varying the ground-state atom density and n.

II. EXPERIMENT

We cool and trap ^{85}Rb atoms in a MOT with an atom-cloud full diameter of ≈ 1 mm using a magnetic-field gradient of 30 G/cm. Via shadow imaging we determine MOT densities and atom numbers to be $\sim 4\times 10^{10}$ cm^{-3} and $\sim 5\times 10^6$. To enhance the atom density, we implement an optical dipole trap via a 5 W ytterbium fiber laser (wavelength 1064 nm) with an intensity profile full width at half maximum (FWHM) of 16 μm sent through the center of the MOT cloud. Typical densities and atom numbers are about 4×10^{11} cm^{-3} and 3×10^4, respectively. The MOT light overlaps the dipole trap light in time for 30 ms, after which the MOT light is turned off. The dipole trap is left on for another 38 ms allowing any atoms not collected in the dipole trap to fall away. The dipole trap is then switched off to avoid any light shift effects on the Rydberg transition energies during optical excitation. We controllably vary the ground-state atom density by adjusting the delay between the shutoff of the dipole trap light and optical excitation. Shadow images illustrating the density evolution as a function of this delay time are shown in Fig. 1(a). Quoted densities are peak densities at the center of the excitation region and have an uncertainty of approximately 20%. Since most of the uncertainty results from diffraction in the shadow imaging system, the quoted densities are more likely underestimated than overestimated.

We prepare atoms in $nD_{5/2}$ Rydberg states using the two-photon excitation process $5S_{1/2} \rightarrow 5P_{3/2} \rightarrow nD_{5/2}$. The excitation is realized with the application of two coincident, counterpropagating, narrow-linewidth, resonant laser pulses. The peak Rabi frequency of the lower transition is 3.5 MHz, as calculated from measurements of Autler-Townes splitting data [21]. The upper transition pulse is focused into the MOT with a FWHM of the intensity profile equal to 19 μm $\pm$ 1 μm, resulting in a Rabi frequency of ≈ 3 MHz. Excitation pulses have a linewidth of <2 MHz and FWHM intensity duration of 100 ns. After a delay time of 100 ns we apply a state-selective field ionization (SSFI) ramp to measure the distribution of produced Rydberg states. The field ionization ramp is shown in Fig. 1(b) (right axis).

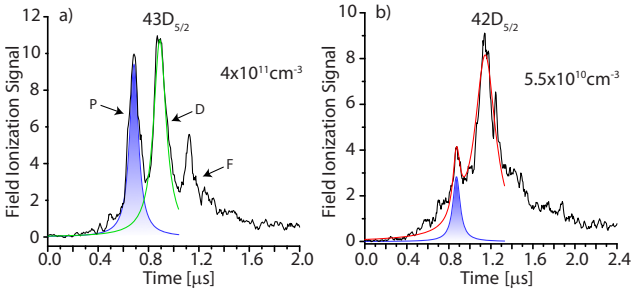

FIG. 2. (Color online) Lorentzian fits for two typical experimental data points. The shaded blue areas are Lorentzian fits to the P signals. (a) Excitation of $43D_{5/2}$ at high density. The individual Lorentzians shown are for the P and D signals. (b) Fitting for nonresonant states ($n \neq 43$). To illustrate the overall agreement of the fit with the experimental results, we show the P signal Lorentzian along with the sum of the Lorentzians.

Figure 1(b) shows measured normalized state-selective electron signals for the state $43D_{5/2}$ for three ground-state atom densities. The signals for the three states that compose the interaction channel given in Eq. (1) are labeled. The lowest-density spectrum (C) contains almost exclusively $43D_{5/2}$ atoms. However, we observe an increasing admixture of $45P_{3/2}$ and $41F_{7/2}$ states as the density increases (A and B), reaching approximately 50% in case A.

We determined state-mixing fractions (number of atoms detected in P and F states divided by the total number of Rydberg excitations) over a range of densities when the laser fields are tuned to excite $nD_{5/2}$ Rydberg levels. To determine the state mixing fraction, we fit the measured spectra to Lorentzians, which were found to give the best empirical fit to the data. Examples of the fits are shown in Fig. 2. Because the $41F_{7/2}$ state ionizes over a much larger range of electric field values than either $45P_{3/2}$ or $43D_{5/2}$ [22], the best quantitative measure of the amount of mixing is given by twice the integral of the region over which the P state ionizes divided by the total integral of the SSFI spectrum. In the vicinity of the Förster resonance at $n=43$, we find that as many as 50% of the excited Rydberg atoms are detected in the $(n-2)F_{7/2}$ and $(n+2)P_{3/2}$ states. Considering the narrow bandwidth (~ 2 MHz) and the short excitation and interaction times (~ 100 ns), this is a surprisingly large mixing fraction. Previous simulations of such conditions, involving two or three atoms at fixed positions, have given mixing fractions of the order of only a few percent [18]. The large mixing fraction cannot be explained by dynamical effects,

since the Rydberg atoms do not move on the time scale of the experiment. The linewidth of the excitation laser is much too narrow (<2 MHz) to excite the product states directly. Moreover, Stark mixing due to free charges can be excluded, because even at the highest densities we observe only an extremely small free electron signal at the onset of the field ionization ramp (less than 1% of the total area of the SSFI signal).

III. THEORY

In order to understand the origin of the observed large state-mixing fractions, we performed extensive many-body simulations by numerically solving the underlying Schrödinger equation for excitation dynamics in the frozen Rydberg gas. In an ensemble of N atoms at positions $\mathbf{r}_i$ the excitation dynamics in the frozen gas is governed by the laser coupling between the atomic ground-state (g) and the excited $nD_{5/2}$ state $\hat{H}_{\mathrm{L}}=\frac{\Omega}{2}\Sigma_i\hat{\sigma}^i_{\mathrm{dg}}+\hat{\sigma}^i_{\mathrm{gd}}$ and the interaction Hamiltonian

$$\hat{H}_{\mathrm{I}}=\sum_{i\neq j}\frac{\hbar}{2}(V^{\mathrm{pf}}_{ij}\hat{\sigma}^i_{\mathrm{dp}}\hat{\sigma}^j_{\mathrm{df}}+\mathrm{H.c.})+\hbar V^{\mathrm{pp}}_{ij}\hat{\sigma}^i_{\mathrm{pd}}\hat{\sigma}^j_{\mathrm{dp}}+\hbar V^{\mathrm{ff}}_{ij}\hat{\sigma}^i_{\mathrm{fd}}\hat{\sigma}^j_{\mathrm{df}}+\sum_i E_{\mathrm{p}}\hat{\sigma}^i_{\mathrm{pp}}+E_{\mathrm{f}}\hat{\sigma}^i_{\mathrm{ff}},\tag{3}$$

where the operator $\hat{\sigma}^i_{\alpha\beta}$ transfers the ith atom from state $|\beta\rangle$ to $|\alpha\rangle$ ($\alpha,\beta=d,p,f$), $V^{\alpha\beta}_{ij}=\mu_{d\alpha}\mu_{d\beta}/4\pi\hbar\epsilon_0 r^3_{ij}$ denotes the corresponding dipole coupling between two atoms and $E_{\mathrm{p(f)}}$ are the energy detunings of the $P_{3/2}$ ($F_{7/2}$) states, with $E_{\mathrm{p}}+E_{\mathrm{f}}=\hbar\Delta$. We reduce the complexity of the calculation by restricting our simulations to the overlap region of the atomic cloud and the excitation laser and by scaling the overall volume by a factor $\epsilon<1$. Our model gas typically still contains a few hundred atoms, corresponding to $\sim 10^{100}$ N-atom states. To reduce this large number of states, we expand the wave function in terms of excitation numbers to obtain evolution equations for the amplitudes $C^{i_1\ldots i_m}_{\alpha_{i_1}\ldots\alpha_{i_m}}$, corresponding to configurations of m Rydberg atoms at positions $\mathbf{r}_{i_1},\ldots,\mathbf{r}_{i_m}$ in states $|\alpha_{i_1},\ldots,\alpha_{i_m}\rangle$. If a given excited state configuration contains Rydberg atom pairs with a distance smaller than a blockade radius, R_{bl}, the corresponding amplitude is set equal to zero and its dynamics is discarded. In this way, the dipole blockade not only reduces the number of relevant many-body states but also limits the number of excitable Rydberg atoms, which allows us to truncate the expansion at a maximum excitation number, $m_{\max}$. Several steps are taken to ensure that our results are not distorted by these measures to reduce the number of basis states. The value of R_{bl} is taken sufficiently small that the results are independent of its precise value. We also increase the relative scaling factor ϵ and the maximally allowed excitation number, $m_{\max}$, until our calculated excitation fractions converge. Typical final values of ϵ and $m_{\max}$ are about 0.5 and 5, respectively.

We emphasize that such complete basis many-body theory (CBMBT) simulations fully account for the N-body Rydberg state exchange dynamics. In contrast, the aforementioned approaches based on an effective pairwise interaction Hamiltonian $\hat{H}_{\mathrm{I}}=\Sigma_{i<j}\hbar U_{ij}\hat{\sigma}^i_{\mathrm{ee}}\hat{\sigma}^i_{\mathrm{ee}}$ turn out to provide an approximate description only. There, the many-body level shift is composed of the pairwise interaction potentials of the type in Eq. (2) between Rydberg atoms. In terms of the original states the projectors $\hat{\sigma}^i_{\mathrm{ee}}$ are given by $\hat{\sigma}^i_{\mathrm{ee}}=1-\hat{\sigma}^i_{\mathrm{gg}}$. In the limit where the laser-bandwidth $\delta\nu$ is smaller than the frequency defect Δ, we can establish the connection between the CBMBT and an effective pairwise Hamiltonian. The original Hamiltonian from Eq. (3) can be re-expressed in a basis set of many-body states with k Rydberg excitations, $\{|e_{i_1},\ldots,e_{i_k},g_{i_{k+1}},\ldots,g_{i_N}\rangle\}$, where the excited state contributions, e, are coherent mixtures of d, p, and f components for the case that two or more excitations exist. The state $|e_{i_1},\ldots,e_{i_k},g_{i_{k+1}},\ldots,g_{i_N}\rangle$ asymptotically connects to $|d_{i_1},\ldots,d_{i_k},g_{i_{k+1}},\ldots,g_{i_N}\rangle$ as $V_{ij}\to 0$, provided that $\Delta/\delta\nu$ is sufficiently large to prevent population of the other states. The mixing fraction of these states is $2k^{-1}\Sigma_{n<m}V^2_{i_n i_m}/(\Delta^2+\Sigma_{n<m}V^2_{i_n i_m})$. In this limit, the effective Hamiltonian for these states can be written as a series of many-body potentials,

$$\hat{H}_{\mathrm{I}}\approx\sum_{i<j}\hbar W^{(2)}_{ij}\hat{\sigma}^i_{\mathrm{ee}}\hat{\sigma}^j_{\mathrm{ee}}+\sum_{i<j<k}\hbar W^{(3)}_{ijk}\hat{\sigma}^i_{\mathrm{ee}}\hat{\sigma}^j_{\mathrm{ee}}\hat{\sigma}^k_{\mathrm{ee}}+\ldots,\tag{4}$$

where the two-body potentials $W^{(2)}_{ij}$ are identical to the U_{ij} in Eq. (2). The $W^{(2)}_{ij}$ are obtained by diagonalizing each two-atom subspace. The higher-order k-body corrections are smaller by a factor of order $|V_{\max}/\Delta|^{k-2}$, where $V_{\max}=\max V^{\alpha\beta}_{ij}$ is the largest dipole coupling in the system. Consequently, the use of pairwise potentials is valid only when $V_{\max}/\Delta\ll 1$. If $V_{\max}/\Delta\gtrsim 1$, higher-order interactions become important and the expansion Eq. (4) must be extended up to the maximum number of excited Rydberg atoms.

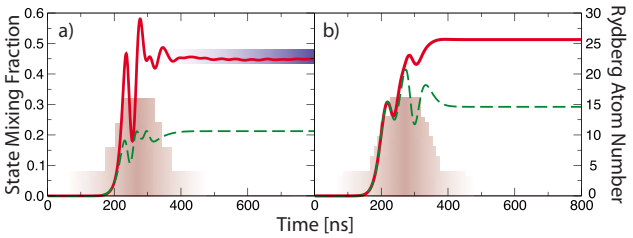

FIG. 3. (Color online) Time evolution of theoretical results for a peak density of 4×10^{11} cm^{-3} and for the state $43D_{5/2}$. The shaded curve illustrates the Gaussian envelope of the excitation pulse having a peak Rabi frequency of 3 MHz. The solid lines show the calculated time evolution obtained from the CBMBT and the dashed lines show the evolution obtained with theory based on sums over pairwise interactions. (a) Theoretical state mixing fraction calculated via the two presented theories and experimental result for the final mixing value shown as a horizontal bar. The width of the bar reflects experimental uncertainty. (b) Theoretical Rydberg excitation number.

Figure 3(a) shows a comparison of measured and calculated state mixing fractions for $n=43$ at a density of $\rho=4\times 10^{11}$ cm^{-3}. There is good agreement with the CBMBT simulations, while the corresponding pairwise result significantly underestimates the state-mixing fraction. By setting $V^{\mathrm{pp}}_{ij}=V^{\mathrm{ff}}_{ij}=0$ we also investigated the effect of the always resonant "hopping" reactions of the type $dp\to pd$, etc. Inter-

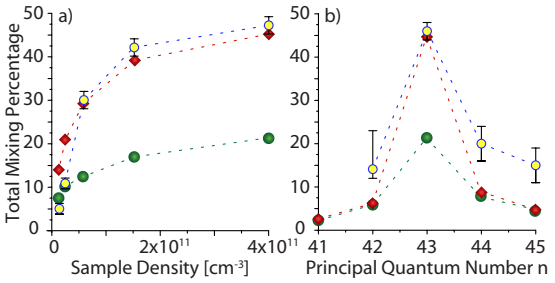

FIG. 4. (Color online) Comparison of mixing predicted by theory based on sums over pairwise interactions (green circles), CBMBT (red diamonds), and experimental results (blue line with open circles). (a) Mixing vs density for excitation of $43D_{5/2}$. (b) Mixing vs principal quantum number n for excitation of states near the resonance of Eq. (1). Error bars are given by the uncertainty in fit parameters as discussed in the text.

estingly, the latter have little effect on the average state-mixing dynamics, leaving the amount of final product states practically unaffected. Additionally, the CBMBT predicts nearly a factor of 2 more Rydberg excitations, as shown in Fig. 3(b). The higher-order interactions derived in Eq. (4) can thus have a considerable effect on the dipole blockade, and in the present case lead to a drastic reduction in its efficiency. The number of Rydberg excitations *detected* in our experiment is typically ~15. The uncertainty in detection efficiency limits our ability to compare experimental and theoretical Rydberg atom excitation numbers. Commonly quoted values of the detection efficiency for microchannel plates range from 30%–70%, corresponding to a range of 21–50 actual excitations, which compares with our theoretical value of 25.

Changing the gas density and/or the principal quantum number of excited Rydberg atoms allows us to tune through a range of dipole coupling strengths as well as energy defects, $\hbar\Delta$. Figure 4(a) shows the measured state mixing fractions for a range of atomic densities stretching over more than an order of magnitude. There is good agreement with the CBMBT simulations, while the state-mixing fractions predicted by the pairwise interaction approach are consistently too low. The results of the two theories converge only at very low densities.

At a given density ρ, the Wigner-Seitz radius $a=(4\pi\rho/3)^{-1/3}$ provides an estimate for the average interatomic distance. The condition $\mu_{\mathrm{dp}}\mu_{\mathrm{df}}/4\pi\epsilon_0 a^3 > \hbar\Delta$ defines the domain where the CBMBT must be used. For $n=43$, this threshold occurs at densities as low as about 10^9 cm^{-3}. For a fixed density chosen to be much greater than this value, the transition between the perturbative (pairwise potential) and nonperturbative (CBMBT) limits can be studied by varying Δ. This is accomplished by exciting $nD_{5/2}$ states with n values in the vicinity of the Förster resonance ($n=43$). Figure 4(b) shows a strongly resonant dependence of the state mixing on the principal quantum number, in reasonable agreement with our CBMBT calculations. Away from resonance both calculations produce very similar results, demonstrating that the perturbative approach involving sums over pairwise level shifts becomes applicable in the limit of off-resonant van der Waals-type interactions. We also note that from the approximate symmetry of the curve in Fig. 4(b) it follows that the mixing observed in our work is not due to an adiabatic crossing behavior studied in Ref. [23].

IV. DISCUSSION

Interactions of Rybderg atoms have been studied in a number of past papers (see for example [16,17] and more recently [8,19,24]).

In [16,17], line broadening in a frozen Rydberg gas was reported. Both observations where explained by energy exchange between two close-lying Rydberg atoms and resonant excitation "hopping" that transports the product states away from the primary pair. Our experiments, together with the presented theory, show that such simplified few-body considerations do not apply for dense gases near Förster resonances. For example, we find that excitation hopping, which was previously suggested [16,17] as a major factor leading to state mixing, does not affect the excitation dynamics for our experimental conditions. This has also been discussed explicitly in recent work [8], where a detailed model of these early experiments is presented. The simulations of [8] give a qualitative description of the experiments [16,17]. Regarding the relationship of these results to our work, we conclude that excitation hopping plays an insignificant role relative to that of the Förster resonance.

Earlier, similar calculations together with time resolved measurements of state mixing have been reported in [19]. Our observed large state mixing fractions after a short time of 100 ns may appear surprising in light of the results of Ref. [19]. In Ref. [19], it was shown that two-atom calculations already reproduce essential features of corresponding simulations with ten atoms; both the initial increase as well as the asymptotic long-time value were nearly identical. We note that in contrast to findings of [8], the simulation results and the experiments presented in Ref. [19] agree well with each other. This may suggest that many-body interaction effects are not crucially important for the final mixing fractions at the densities considered in Ref. [19]. In contrast, at the higher densities realized in the present work, experimental results and the corresponding two-atom calculation differ by more than an order of magnitude from each other. This demonstrates that many-body interactions of the type given in Eq. (4), for the case of $m_{\max}>2$, do not simply give small corrections to the excitation dynamics, but in fact substantially affect the state mixing.

In previous work ([8,19,24]), the excitation process and the state mixing have been considered as two separate processes (without time overlap). Here we show that an almost complete redistribution to product states (50%) takes place on a rapid time scale and is already very effective while the laser excitation is still in progress. This demonstrates that at high atom densities the state mixing process cannot be separated from the laser excitation to Rydberg states. Rydberg atoms become highly correlated and build up entanglement during the excitation process due to the dipole blockade. A simultaneous theoretical description of both processes requires several hundred atoms, substantially larger than in previous simulations [8,19] in which state mixing has been

considered as a separate process (occurring after the excitation is complete). The simulations show that the resulting interplay between laser excitation and excitation exchange between atoms plays a crucial role for the state mixing as well as for the total fraction of Rydberg atoms, i.e., the blockade efficiency. This fact and the rapid state mixing during laser excitation should generally be important for interpretations of dense Rydberg gas experiments in which strong, resonant interaction effects are studied.

Perhaps most significantly, we explicitly show that higher-order particle interactions of the type given in Eq. (4) play a profound role in the excitation dynamics of dense Rydberg gases. The comparison of our simulation results using only the first term of Eq. (4) and the CBMBT simulations [see Fig. 3(b)] clearly reveals the effect of higher-order interactions, leading to a significant reduction in the dipole blockade efficiency. Our state mixing measurements together with the theoretical simulation show that simplified pictures based on pairwise interaction-induced level shifts do not fully reflect the dipole-blocked excitation dynamics at Förster resonances [25].

In Ref. [26] it was shown that, under certain angular momentum conditions, specific molecular Rydberg levels do not exhibit a strong energy shift. In our experiment, these so-called Förster zero states would lead to the excitation of more $D_{5/2}$ atoms and thus a reduction in state-mixing fractions. Thus, Förster zero states do not present a mechanism by which more state mixing could be generated. The large state-mixing fractions observed in our work suggest that Förster zero states do not strongly influence our experimental results.

V. CONCLUSION

In summary, we have presented an experimental and theoretical study of the collective excitation dynamics in a dense, frozen Rydberg gas. Measuring the redistribution of Rydberg states induced by strong dipole-dipole coupling between adjacent levels, we find surprisingly efficient state mixing on a time scale as short as 100 ns. A comparison with numerical simulations reveals that a complete many-body basis is needed to account for the complex quantum many-body dynamics resulting from Förster processes.

These results demonstrate that cold Rydberg gases provide an experimentally accessible system to study exotic, nonperturbative many-body dynamics. For example, external electric [13] or optical fields [27] permit a continuous variation in the energy defect and hence a controlled study of the interesting transition region between on-resonant and off-resonant interactions.

ACKNOWLEDGMENTS

This work was supported in part by NSF through a grant to ITAMP and Grants No. PHY-0114336 and No. PHY-0555520. K.C.Y. acknowledges support from NDSEG.

[1] T. Cubel Liebisch, A. Reinhard, P. R. Berman, and G. Raithel, Phys. Rev. Lett. **95**, 253002 (2005).
[2] T. Vogt, M. Viteau, A. Chotia, J. Zhao, D. Comparat, and P. Pillet, Phys. Rev. Lett. **99**, 073002 (2007).
[3] D. Tong, S. M. Farooqi, J. Stanojevic, S. Krishnan, Y. P. Zhang, R. Cote, E. E. Eyler, and P. L. Gould, Phys. Rev. Lett. **93**, 063001 (2004).
[4] U. Raitzsch, V. Bendkowsky, R. Heidemann, B. Butscher, R. Low, and T. Pfau, Phys. Rev. Lett. **100**, 013002 (2008).
[5] R. Heidemann, U. Raitzsch, V. Bendkowsky, B. Butscher, R. Low, L. Santos, and T. Pfau, Phys. Rev. Lett. **99**, 163601 (2007).
[6] J. V. Hernández and F. Robicheaux, J. Phys. B **41**, 045301 (2008).
[7] C. Ates, T. Pohl, T. Pattard, and J. M. Rost, Phys. Rev. A **76**, 013413 (2007).
[8] B. Sun and F. Robicheaux, Phys. Rev. A **78**, 040701(R) (2008).
[9] T. Förster, Z. Naturforsch. A **4**, 321 (1949).
[10] S. Jang, M. D. Newton, and R. J. Silbey, Phys. Rev. Lett. **92**, 218301 (2004).
[11] K. Becker *et al.*, Nature Mater. **5**, 777 (2006).
[12] M. D. Lukin, M. Fleischhauer, R. Cote, L. M. Duan, D. Jaksch, J. I. Cirac, and P. Zoller, Phys. Rev. Lett. **87**, 037901 (2001).
[13] T. Vogt, M. Viteau, J. Zhao, A. Chotia, D. Comparat, and P. Pillet, Phys. Rev. Lett. **97**, 083003 (2006).
[14] J. V. Hernández and F. Robicheaux, J. Phys. B **39**, 4883 (2006).
[15] J. Stanojevic and R. Côté, e-print arXiv:0801.2396.
[16] W. R. Anderson, J. R. Veale, and T. F. Gallagher, Phys. Rev. Lett. **80**, 249 (1998).
[17] I. Mourachko, D. Comparat, F. de Tomasi, A. Fioretti, P. Nosbaum, V. M. Akulin, and P. Pillet, Phys. Rev. Lett. **80**, 253 (1998).
[18] A. Reinhard, T. Cubel Liebisch, K. C. Younge, P. R. Berman, and G. Raithel, Phys. Rev. Lett. **100**, 123007 (2008).
[19] S. Westermann *et al.*, Eur. Phys. J. D **40**, 37 (2006).
[20] M. Reetz-Lamour, T. Amthor, J. Deiglmayr, and M. Weidemüller, Phys. Rev. Lett. **100**, 253001 (2008).
[21] B. K. Teo, D. Feldbaum, T. Cubel, J. R. Guest, P. R. Berman, and G. Raithel, Phys. Rev. A **68**, 053407 (2003).
[22] T. F. Gallagher, *Rydberg Atoms* (Cambridge University Press, Cambridge, 1994).
[23] J. Han and T. F. Gallagher, Phys. Rev. A **77**, 015404 (2008).
[24] C. S. E. van Ditzhuijzen, A. F. Koenderink, J. V. Hernandez, F. Robicheaux, L. D. Noordam, and H. B. van Linden van den Heuvell, Phys. Rev. Lett. **100**, 243201 (2008).
[25] T. Pohl and P. R. Berman, Phys. Rev. Lett. **102**, 013004 (2009).
[26] T. G. Walker and M. Saffman, J. Phys. B **38**, S309 (2005).
[27] P. Bohlouli-Zanjani, J. A. Petrus, and J. D. D. Martin, Phys. Rev. Lett. **98**, 203005 (2007).